

On Adaptive Frequency Sampling for Data-driven Model Order Reduction Applied to Antenna Responses

Lucas Åkerstedt, Darwin Blanco, and B. L. G. Jonsson

Abstract—Frequency domain sweeps of array antennas are well-known to be time-intensive, and different surrogate models have been used to improve the performance. Data-driven model order reduction algorithms, such as the Loewner framework and vector fitting, can be integrated with these adaptive error estimates, in an iterative algorithm, to reduce the number of full-wave simulations required to accurately capture the requested frequency behavior of multiport array antennas. In this work, we propose two novel adaptive methods exploiting a block matrix function which is a key part of the Loewner framework generating system approach. The first algorithm leverages an inherent matrix parameter freedom in the block matrix function to identify frequency points with large errors, whereas the second utilizes the condition number of the block matrix function. Both methods effectively provide frequency domain error estimates, which are essential for improved performance. Numerical experiments on multiport array antenna S-parameters demonstrate the effectiveness of our proposed algorithms within the Loewner framework, where the proposed algorithms reach the smallest errors for the smallest number of frequency points chosen.

Index Terms—Adaptive frequency sampling, adaptive interpolation, frequency domain simulations, Loewner framework, frequency sweeps, S-parameters.

I. INTRODUCTION

SIMULATING antenna array responses in the frequency domain is often time-consuming. For example, in Method of Moments (MoM) one needs to calculate the impedance matrix and solve a linear system for each frequency point. The total required time depends on the electrical size, the number of antenna ports, and the frequency band of the problem. Furthermore, the simulation challenges become even larger when out-of-band properties are needed [1].

One method to speed up the process is to determine fewer frequency points in combination with a Model Order Reduction (MOR) process [2], [3]. Methods that address the matrix completion time include using the Toeplitz structure [4] and methods to solve the linear system fast include iterative methods [5].

A key part, on which this work is based on, is the Loewner framework, a method that has been shown to efficiently approximate solutions to partial differential equations and nonlinear systems [6], [7]. Other algorithms and methods for system approximation include Cauchy interpolation [8], [9]

and vector fitting [10], [11]. The Loewner framework and vector fitting are categorized as *non-intrusive* (or *data-driven*) MOR methods [12]. Non-intrusive methods use only the input and output data of a system, and not any prior physical knowledge of a system [13]. In this paper, the two data-driven MOR methods, the Loewner framework and vector fitting, are used and compared.

Comparisons between the Loewner framework and vector fitting have been conducted in [12], [14]–[16]. These papers compare the MOR methods on various frequency responses. Interestingly, there are no comparisons between the methods for antenna frequency responses that we have found. The individual use of vector fitting and Loewner matrix-based system representation in an antenna context has, however, been carried out before in [17], [18], and in [19]–[21], respectively. One of the contributions of this paper is a comparison of the Loewner framework and vector fitting, when specifically applied to array antenna responses.

Using a system approximation method in an iterative sense to adaptively choose frequency samples for the construction of a system model is known as *adaptive frequency sampling* [22]–[24]. Prior works on adaptive frequency sampling algorithms for non-intrusive MOR include the greedy algorithm by Pradovera [25], the scheme by Vuillemin and Poussot-Vassal [26], and the greedy algorithm by Cherifi *et al.*, [27]. These algorithms aim to select as few frequency samples as possible while still obtaining an accurate system approximation.

In this paper, we introduce two novel adaptive frequency sampling algorithms based on the *generating system*-approach from [16]. These adaptive methods are tested on antenna array responses and compared with the adaptive methods from [25] and [26], as well as equidistant distributions using the Loewner framework and vector fitting. From the comparison, the two novel frequency sampling algorithms yield the best performance in terms of accuracy as a function of the number of frequency samples used, on the examined systems. Additionally, an accurate, novel, error estimator of the system approximation generated using the Loewner framework is presented. System representations are associated with an error. Accurate estimation of the introduced error is essential in an adaptive frequency sampling scheme. In summary, an improved framework is presented where frequency points are chosen in an iterative process with MoM to yield an error-controlled system representation of the antenna response. A different approach to a similar problem is presented in [28].

This paper is organized as follows. The theory of scalar vec-

tor fitting and the Loewner framework is shown in Section II. Section III introduces the theory of the adaptive sampling algorithms tested in this paper. In Section IV, the adaptive frequency sampling algorithms are tested on various antenna responses. Lastly, Section V concludes the paper.

II. THEORY

A. Vector Fitting

Vector fitting is well described in [10], [13]. We repeat the main steps in the scalar case for completeness. Let $s \in \mathbb{C}$ be the complex Laplace variable such that $s = j\omega$, where $\omega \in \mathbb{R}$ is the angular frequency. Vector fitting approximates the scalar function $S(s)$ as a rational function $h(s)$,

$$h(s) = \sum_{n=1}^N \frac{r_n}{s - a_n} + d + se, \quad (1)$$

where $r_n \in \mathbb{C}$ are the residues, $a_n \in \mathbb{C}$ are the poles, and $d, e \in \mathbb{C}$ are the asymptotic expansion coefficients. Solving for the coefficients in (1) is a non-linear problem that is linearized and solved iteratively by first creating the augmented problem

$$\begin{cases} \sigma(s)h(s) \approx \sum_{n=1}^N \frac{r_n}{s - \tilde{a}_n} + d + se \\ \sigma(s) \approx \sum_{n=1}^N \frac{\tilde{r}_n}{s - \tilde{a}_n} + 1 \end{cases}, \quad (2)$$

where \tilde{a}_n are the starting poles and are set according to a heuristic scheme. Multiplying $\sigma(s)$ from (2) with $h(s)$ and rearranging yields

$$\sum_{n=1}^N \frac{r_n}{s - \tilde{a}_n} + d + se - h(s) \sum_{n=1}^N \frac{\tilde{r}_n}{s - \tilde{a}_n} \approx h(s). \quad (3)$$

Given $\{s_i, S(s_i)\}_{i=1}^{N_s}$ and $h(s_i) = S(s_i)$, (3) yields a linear system that is solved in the least square sense. Solving the linear system yields the approximative solution to the unknown coefficients, r_n, \tilde{r}_n, d, e . Given $\{\tilde{r}_n\}$ a new set of poles $\{\tilde{a}_n\}$ are obtained by solving the eigenvalue problem

$$\{\tilde{a}_n\} = \text{eig}(\tilde{\mathbf{A}} - \tilde{\mathbf{b}} \cdot \tilde{\mathbf{r}}). \quad (4)$$

Here, $\tilde{\mathbf{A}} = \text{diag}(\tilde{a}_1, \dots, \tilde{a}_N)$, $\tilde{\mathbf{b}} = [1, \dots, 1]^T$, and $\tilde{\mathbf{r}} = [\tilde{r}_1, \dots, \tilde{r}_N]^T$. The procedure (3) - (4) is repeated for a number of iterations. The final set of poles is inserted into (1), which leaves a linear problem, solved in the least square sense to obtain the final set of residues $\{r_n\}$ and the asymptotic coefficients d and e . For a generalization to the matrix case, see [13].

B. The Block Loewner Framework

With the block Loewner framework [16], [29], the transfer function matrix at each sample is used as data. Given the discrete data set $P = \{s_i, \mathbf{S}(s_i)\}_{i=1}^{N_s}$, where $\mathbf{S}(s_i) \in \mathbb{C}^{p \times m}$, the set is partitioned into two disjoint sets

$$\begin{cases} P_c = \{(\lambda_i, \mathbf{w}_i) : i = 1, \dots, k\} \\ P_r = \{(\mu_j, \mathbf{v}_j) : j = 1, \dots, q\} \end{cases}, \quad (5)$$

where

$$\left. \begin{aligned} \lambda_i &= s_i, & \mathbf{w}_i &= \mathbf{S}(\lambda_i), & i &= 1, \dots, k \\ \mu_j &= s_{k+j}, & \mathbf{v}_j &= \mathbf{S}(\mu_j), & j &= 1, \dots, q \end{aligned} \right\}, \quad k + q = N_s. \quad (6)$$

In this paper, we use *alternate splitting* [30] for partitioning the set P into P_c and P_r . With alternate splitting, the frequencies s_i are sorted according to their angular frequency ω_i . Then, every other frequency is said to belong to P_c . The remaining frequencies are said to belong to P_r .

From the two data sets P_c and P_r , the left and right data (or more precisely, row and column data) are constructed as follows:

$$\left. \begin{aligned} \mathbf{A} &= \text{diag}(\lambda_1, \dots, \lambda_k) \otimes \mathbb{I}_m \in \mathbb{C}^{(mk) \times (mk)} \\ \mathbf{R} &= [\mathbb{I}_m, \dots, \mathbb{I}_m] \in \mathbb{C}^{m \times (mk)} \\ \mathbf{W} &= [\mathbf{w}_1, \dots, \mathbf{w}_k] \in \mathbb{C}^{p \times (mk)} \end{aligned} \right\}, \quad (7)$$

where \mathbb{I}_m is the $m \times m$ identity matrix, and \otimes indicates the Kronecker product.

From the data set P_r , the left data (row data) is constructed

$$\left. \begin{aligned} \mathbf{M} &= \text{diag}(\mu_1, \dots, \mu_q) \otimes \mathbb{I}_p \in \mathbb{C}^{(pq) \times (pq)} \\ \mathbf{L} &= [\mathbb{I}_p, \dots, \mathbb{I}_p]^T \in \mathbb{C}^{(pq) \times p} \\ \mathbf{V} &= [\mathbf{v}_1^T, \dots, \mathbf{v}_q^T]^T \in \mathbb{C}^{(pq) \times m} \end{aligned} \right\}. \quad (8)$$

For other approaches to constructing the left and right data, e.g. *tangential* interpolation, see [16], [29], [31].

From the left and right data, the *block Loewner matrix* is constructed

$$\mathbb{L} = \begin{bmatrix} \frac{\mathbf{v}_1 - \mathbf{w}_1}{\mu_1 - \lambda_1} & \dots & \frac{\mathbf{v}_1 - \mathbf{w}_k}{\mu_1 - \lambda_k} \\ \vdots & \ddots & \vdots \\ \frac{\mathbf{v}_q - \mathbf{w}_1}{\mu_q - \lambda_1} & \dots & \frac{\mathbf{v}_q - \mathbf{w}_k}{\mu_q - \lambda_k} \end{bmatrix} \in \mathbb{C}^{(pq) \times (mk)}. \quad (9)$$

Within the Loewner framework, there exist at least three approaches for constructing a system representation $\mathbf{H}(s)$, such that $\mathbf{H}(s) \approx \mathbf{S}(s)$. For the first approach [31, Sec 4], the surrogate model $\mathbf{H}(s)$ is constructed using the state space representation

$$\mathbf{H}(s) = \mathbf{C}(s\mathbb{I} - \mathbf{A})^{-1}\mathbf{B} + \mathbf{D}, \quad (10)$$

where the state space matrices $\mathbf{A}, \mathbf{B}, \mathbf{C}, \mathbf{D}$ are given by

$$\left(\begin{array}{c|c} \mathbf{A} & \mathbf{B} \\ \hline \mathbf{C} & \mathbf{D} \end{array} \right) = \left(\begin{array}{c|c} \mathbf{A} + \mathbb{L}^\#(\mathbf{V} - \mathbf{LD}) & \mathbb{L}^\#(\mathbf{V} - \mathbf{LD}) \\ \hline -(\mathbf{W} - \mathbf{DR}) & \mathbf{D} \end{array} \right), \quad (11)$$

where \mathbf{D} is arbitrary, and $\mathbb{L}^\#$ is the right inverse of \mathbb{L} (and can be calculated by, e.g. the Penrose-Moore inverse).

The second method of constructing the surrogate model is called the *generating system* approach [16], [29]. Here, the block matrix function $\Theta(s)$, or its inverse $\bar{\Theta}(s)$, is constructed to generate the surrogate model:

$$\begin{aligned} \mathbf{H}(s) &= [\Theta_{11}(s)\mathbf{G}_1(s) - \Theta_{12}(s)\mathbf{G}_2(s)] \\ &\quad [-\Theta_{21}(s)\mathbf{G}_1(s) + \Theta_{22}(s)\mathbf{G}_2(s)]^{-1}, \end{aligned} \quad (12)$$

or

$$\begin{aligned} \mathbf{H}(s) &= [\mathbf{G}_1(s)\bar{\Theta}_{11}(s) + \mathbf{G}_2(s)\bar{\Theta}_{21}(s)] \\ &\quad [\mathbf{G}_1(s)\bar{\Theta}_{12}(s) + \mathbf{G}_2(s)\bar{\Theta}_{22}(s)]^{-1}, \end{aligned} \quad (13)$$

where $\mathbf{G}_1(s)$ and $\mathbf{G}_2(s)$ are arbitrary polynomial matrices [29]. If $k = q$, and \mathbb{L} is invertible, the block matrices $\Theta(s) \in \mathbb{C}^{(p+m) \times (p+m)}$ and $\bar{\Theta}(s) \in \mathbb{C}^{(p+m) \times (p+m)}$ are defined as [16], [29]

$$\begin{aligned} \Theta(s) &= \begin{bmatrix} \mathbb{I}_p & 0 \\ 0 & \mathbb{I}_m \end{bmatrix} + \begin{bmatrix} \mathbf{W} \\ -\mathbf{R} \end{bmatrix} (s\mathbb{L} - \mathbb{L}\mathbf{A})^{-1} \begin{bmatrix} \mathbf{L} & \mathbf{V} \end{bmatrix} \\ &= \begin{bmatrix} \Theta_{11}(s) & \Theta_{12}(s) \\ \Theta_{21}(s) & \Theta_{22}(s) \end{bmatrix}, \end{aligned} \quad (14)$$

and

$$\begin{aligned} \bar{\Theta}(s) &= \begin{bmatrix} \mathbb{I}_p & 0 \\ 0 & \mathbb{I}_m \end{bmatrix} + \begin{bmatrix} -\mathbf{W} \\ \mathbf{R} \end{bmatrix} (s\mathbb{L} - \mathbf{M}\mathbb{L})^{-1} \begin{bmatrix} \mathbf{L} & \mathbf{V} \end{bmatrix} \\ &= \begin{bmatrix} \bar{\Theta}_{11}(s) & \bar{\Theta}_{12}(s) \\ \bar{\Theta}_{21}(s) & \bar{\Theta}_{22}(s) \end{bmatrix}. \end{aligned} \quad (15)$$

The third approach is the barycentric interpolation representation [29]

$$\mathbf{H}(s) = \frac{\sum_{i=1}^k \frac{b_i \mathbf{w}_i}{s - \lambda_i}}{\sum_{i=1}^k \frac{b_i}{s - \lambda_i}}, \quad (16)$$

where b_i are the barycentric coefficients. The barycentric coefficients b_i are obtained by solving the optimization problem [25]

$$\begin{aligned} \text{minimize } & \sum_{j=1}^q \left\| \sum_{i=1}^k b_i \frac{\mathbf{v}_j - \mathbf{w}_i}{\mu_j - \lambda_i} \right\|_F^2 \\ \text{subject to } & \sum_{i=1}^k |b_i|^2 = 1, \end{aligned} \quad (17)$$

where $\|\cdot\|_F$ is the Frobenius norm.

III. FREQUENCY SAMPLING ALGORITHMS

Frequency domain simulations of antennas yield the frequency response calculated at a given discrete set of frequencies. The duration for calculating the frequency response for one frequency point is often quite high for arrays. It is, therefore, desirable to keep the number of frequency points low while still having enough frequency points for the system approximation to accurately resemble the frequency response. Choosing these frequency points in the given frequency band is in this work denoted as *frequency sampling*, [2], [25].

Frequency points may either be sampled in an adaptive or predetermined manner. Predetermined frequency sampling means that a set of frequency points is chosen prior to any frequency domain calculations.

In adaptive frequency sampling, an initial set of frequency samples is iteratively enriched based on an error estimation over a desired frequency band. First, the error estimation is carried out using the available sample points. Then, the frequency response from the surrogate model is examined to determine the largest error and the corresponding frequency point is then added to the available samples. The procedure then continues iteratively until it has reached an estimated error smaller than a given error tolerance or a maximum number of iterations. Some error estimation methods utilize properties of the system representation method, whereas some methods only utilize the data of the constructed model. A general description

of the adaptive frequency sampling algorithms presented here is displayed in Algorithm 1.

The number of frequency points in the initial set varies. In [32], a sparse uniformly sampled set is used, whereas in [25], only one to two frequency points are used in the initial set. In this work, we use only two frequency points in the initial set: the lower and upper-frequency limit of the band of interest.

Throughout this paper, we denote the number of samples *used* for system approximation with N_s . Once the surrogate model is constructed, it can provide a system approximation on a fine grid. This fine grid consists of M_s equidistantly spaced frequency samples in the frequency band of interest, $[f_{\min}, f_{\max}]$. Here, we denote these fine sampled points with s'_ℓ , whereas the samples chosen in an adaptive or predetermined manner are denoted with s_i . Typically, the chosen samples form a subset in the band of interest, i.e., $\{s_i\}_{i=1}^{N_s} \subseteq \{s'_\ell\}_{\ell=1}^{M_s}$, $N_s \leq M_s$, often $N_s \ll M_s$.

Algorithm 1 General adaptive frequency sampling algorithm

Input: Initial set of N samples $\{s_i, \mathbf{S}(s_i)\}_{i=1}^N$

Desired error tolerance: E_{tol}

Number of maximum iterations: N_{max}

Number of points for surrogate model construction: M_s

Band of interest: f_{\min}, f_{\max}

Output: $\mathbf{H}(s'_\ell)$

- 1: Set of samples $\mathcal{S} = \{s_i, \mathbf{S}(s_i)\}_{i=1}^N$
 - 2: Points for surrogate model $\{s'_\ell\}_{\ell=1}^{M_s} = 2\pi j \text{ linspace}(f_{\min}, f_{\max}, M_s)$
 - 3: Initial estimated error: $E_{\text{est}} = \infty$
 - 4: **for** $n = 0, \dots, N_{\text{max}} - 1$ **do**
 - 5: Construct model $\mathbf{H}(s'_\ell)$ with the $N + n$ samples available, for $\ell = 1, \dots, M_s$
 - 6: Estimate error E_{est} of $\mathbf{H}(s'_\ell)$
 - 7: **if** $E_{\text{est}} < E_{\text{tol}}$ **then**
 - 8: Break
 - 9: **end if**
 - 10: Choose next point s_{N+n+1} from the estimated error or by analyzing $\mathbf{H}(s'_\ell)$ (or other system approximation method specific properties)
 - 11: Calculate $\mathbf{S}(s_{N+n+1})$
 - 12: Add sample: $\mathcal{S} \leftarrow \mathcal{S} \cup \{s_{N+n+1}, \mathbf{S}(s_{N+n+1})\}$
 - 13: **end for**
 - 14: **return** $\mathbf{H}(s'_\ell)$
-

For predetermined frequency distributions, any arbitrary distribution of frequency points may be used as long as the choice of points is made before any system approximation is carried out. In this work, we use an equidistant distribution. While an equidistant distribution is not practical in an iterative setting, it serves as a good benchmarking reference.

Each of the proposed methods below, see Section III-B - III-E, utilize different methods to predict the largest error. To compare and quantize the performance of these methods, an error between the constructed surrogate models and the true data is calculated. In this paper, all system approximation and sampling methods are *evaluated* by the Root Mean Square

Error (RMSE), similarly to [12],

$$\text{RMSE} = \left(\frac{1}{M_s} \sum_{\ell=1}^{M_s} \|\mathbf{S}(s'_\ell) - \mathbf{H}(s'_\ell)\|_F^2 \right)^{\frac{1}{2}}, \quad (18)$$

where $\mathbf{S}(s'_\ell)$ is the testing data, and $\mathbf{H}(s'_\ell)$ is the constructed surrogate model. Throughout Section IV, the testing data consists of scattering parameters calculated for a discrete set of frequencies, s'_1, \dots, s'_{M_s} , obtained using commercial full-wave simulation software or an in-house MoM solver. Therefore, the surrogate models are constructed for the same set of discrete frequencies, s'_1, \dots, s'_{M_s} , to relieve the use of (18).

In Section IV we also display the relative error between the testing data and the surrogate models, as a function of frequency. Here, we consider the Frobenius norm of the element-wise relative error, E_{rel} ,

$$E_{\text{rel}}(s'_\ell) = \|\mathbf{E}(s'_\ell)\|_F, \quad E_{ij}(s'_\ell) = \frac{H_{ij}(s'_\ell) - S_{ij}(s'_\ell)}{S_{ij}(s'_\ell) + \delta}, \quad (19)$$

where $\delta = 10^{-15}$.

A. Double-sided Sampling

The transfer function $\mathbf{S}(s)$ of an LTI system is *Positive Real* (the admittance or impedance representation) or *Bounded Real* if and only if the LTI system is passive [13, Th 2.1]. Both a positive real and a bounded real transfer function $\mathbf{S}(s)$ fulfills

$$\mathbf{S}(s)^* = \mathbf{S}(s^*). \quad (20)$$

Given N_s discrete samples on the imaginary axis, $\{\mathbf{j}\omega_i, \mathbf{S}(\mathbf{j}\omega_i)\}_{i=1}^{N_s}$, of a passive LTI system, the passivity may be exploited to obtain additional N_s samples. First, consider the sampled set $\{\mathbf{j}\omega_i, \mathbf{S}(\mathbf{j}\omega_i)\}_{i=1}^{N_s}$. Using (20), with the already sampled set, we obtain the set $\{-\mathbf{j}\omega_i, \mathbf{S}(\mathbf{j}\omega_i)^*\}_{i=1}^{N_s}$. This procedure leaves us with the double amount of samples and is here denoted as *double-sided sampling*. In this work, we use double-sided sampling unless stated otherwise.

B. Vuillemin Adaptive Frequency Sampling

The adaptive frequency sampling algorithm described in [26] is a heuristic scheme that samples the next frequency point according to the strongest dynamic of the current surrogate model. This method identifies the dynamics by finding the peaks and valleys of the current surrogate model. In [26], the method is used together with the Loewner framework.

Considering the general description of adaptive frequency sampling in Algorithm 1, the method in [26] specifies line 10, i.e., the analysis of the surrogate model (or the properties of the system approximation method) to decide the next point to sample. From the current surrogate model, $\mathbf{H}(s'_\ell)$, a scalar function is defined

$$g(\omega_\ell) = \|\mathbf{H}(\mathbf{j}\omega_\ell)\|_2, \quad (21)$$

where $\|\cdot\|_2$ is the ℓ^2 -norm. The discrete frequency corresponding to the largest or lowest value of $g(\omega_\ell)$ is then chosen as the candidate point. If there are no peaks or valleys, the frequency point corresponding to the largest or smallest discrete derivative of $g(\omega_\ell)$ is selected as the candidate point.

C. Pradovera Adaptive Frequency Sampling

Another adaptive sampling algorithm to investigate is the greedy sampling algorithm described by Pradovera in [25]. In [25], an adaptive sampling algorithm is constructed based on the barycentric interpolant representation (see (16)) for the Loewner framework. Pradovera shows that the *relative residual norm* $\rho(s)$ of the surrogate model $\mathbf{H}(s)$ satisfies [25, eq. (10)]

$$\rho(s) = \gamma \left| \sum_{i=1}^k \frac{b_i}{s - \lambda_i} \right|^{-1}, \quad (22)$$

where γ is a frequency-independent constant. Subsequently, the next frequency point is sampled to minimize the magnitude of the norm of the sum in (22). A frequency sampling rule is thus obtained:

$$s_{N_s+1} = \arg \min_s \left| \sum_{i=1}^k \frac{b_i}{s - \lambda_i} \right|. \quad (23)$$

In [25], double sided sampling is used such that $P_c = \{s_i, \mathbf{S}(s_i)\}_{i=1}^{N_s}$, $P_r = \{s_i^*, [\mathbf{S}(s_i)]^*\}_{i=1}^{N_s}$.

D. Loewner Generating System Based Adaptive Sampling I

Here, we propose the first of our two novel adaptive sampling methods. In [16], an adaptive sampling scheme based on the Loewner generating system approach is described. The method from [16] is employed in a context where a large number of samples are already available, e.g., measured S-parameters. There, the goal is to add a number of (already available) samples in each iteration to be used with the Loewner framework to create a reduced order model.

Recall that in this paper, no samples are available in advance. The choice of the next frequency point to sample is driven by the already sampled frequency points. Similarly to [16], we may, however, use the generating system approach to create an adaptive sampling scheme. The underlying philosophy is as follows:

N surrogate models are constructed using the generating function $\Theta(s)$ (or $\bar{\Theta}(s)$, see (14) and (15)) together with a set of different arbitrary matrices $\mathbf{G}_1^{(\tau)}$ and $\mathbf{G}_2^{(\tau)}$, $\tau = 1, 2, \dots, N$. A surrogate model constructed from the matrices $\mathbf{G}_1^{(\tau)}$ and $\mathbf{G}_2^{(\tau)}$ is in this paper denoted by $\mathbf{H}^{(\tau)}(s'_\ell)$. The discrete frequency point for which the surrogate models $\mathbf{H}^{(1, \dots, N)}(s'_\ell)$ differ the most is then selected as the next frequency point to sample. The difference among the models can be calculated in a number of ways. In this paper, the element-wise relative difference is calculated, i.e.,

$$s_{N_s+1} = \arg \max_{\ell, i, j, \tau, \nu} \left| \frac{H_{ij}^{(\tau)}(s'_\ell) - H_{ij}^{(\nu)}(s'_\ell)}{H_{ij}^{(\tau)}(s'_\ell)} \right|. \quad (24)$$

It is, however, possible to perform other sorts of difference calculations, e.g., absolute difference.

The Theta I method relies on the block matrix function $\Theta(s)$ (or $\bar{\Theta}(s)$), which is only defined for when $k = q$ and when \mathbb{L} is invertible. As a consequence, the method must be fed an even number of square matrix samples $\{s_i, \mathbf{S}(s_i)\}_{i=1}^{N_s}$ unless we modify the calculation of the block matrix $\Theta(s)$.

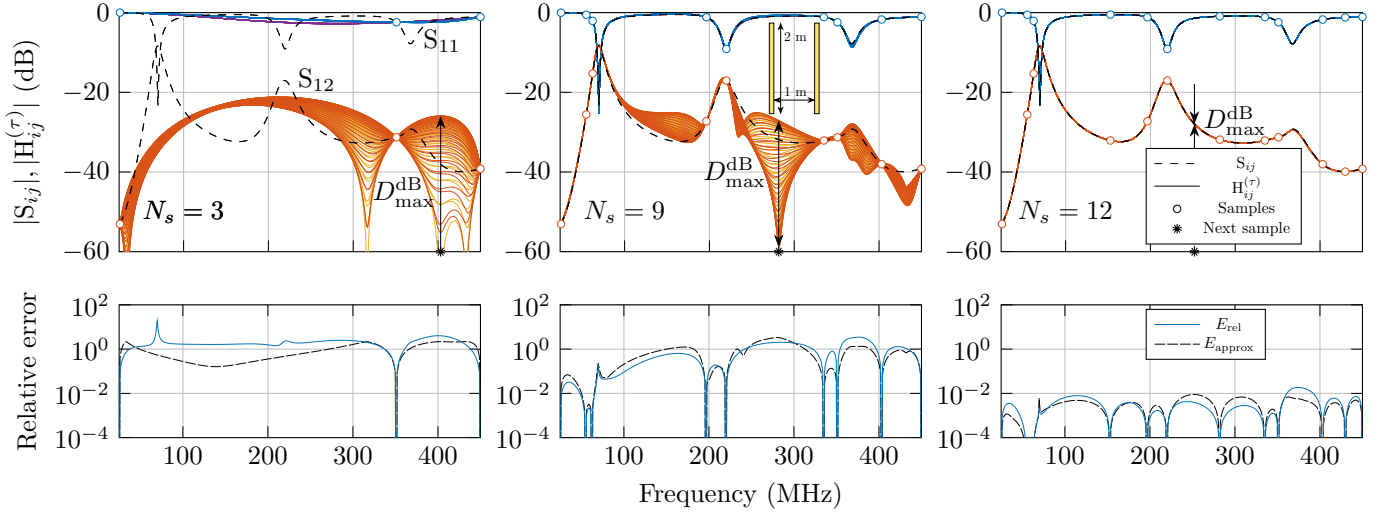


Fig. 1. Forty surrogate models constructed using (12) with the unitary matrices $\mathbf{G}_1^{(\tau)}$ and $\mathbf{G}_2^{(\tau)}$, $\tau = 1, \dots, 40$, for 3, 9, and 12 available samples. The largest relative deviation is highlighted with D_{\max}^{dB} , which decides the next frequency point to sample. In the lower plots, the corresponding relative error (19) and the estimated relative error using (25), are displayed.

Here, we propose three ways of managing an odd number of samples. Either use a pseudo-inverse for the calculation of $(s\mathbb{L} - \mathbb{L}\mathbf{A})^{-1}$, or Split the N_s (N_s being odd) available samples into two groups such that the first group consists of samples $1, 2, \dots, N_s - 1$, and the second group consists of samples $2, 3, \dots, N_s$. The calculation in (24) is then performed on the two groups separately, which yields us two candidate points. Of the two candidate points, the one corresponding to the largest difference among the corresponding surrogate models is chosen. Lastly, the principle of double-sided sampling may be used to always have $2N_s$ samples available. This solution, however, limits us to passive LTI systems only.

With our proposed method, we may *approximate* the relative error E_{rel} by calculating the maximum relative difference among the surrogate models:

$$E_{\text{approx}}(s'_\ell) = \|\tilde{\mathbf{E}}(s'_\ell)\|_F, \quad \tilde{E}_{ij}(s'_\ell) = \max_{\tau, \nu} \frac{1}{p} \left| \frac{H_{ij}^{(\tau)}(s'_\ell) - H_{ij}^{(\nu)}(s'_\ell)}{H_{ij}^{(\tau)}(s'_\ell) + \delta} \right|. \quad (25)$$

In Fig. 1, we display an example of how the adaptive method is used to approximate a given antenna response. Here, the Theta I method is used to approximate the scattering data originating from two 2m long dipole antennas situated 1m apart (see inset of Fig. 1), operating in the frequency band 25 MHz to 450 MHz, with 50 Ω port impedances. For demonstrative purposes, we have chosen our set of matrices $\mathbf{G}_1^{(\tau)}$, and $\mathbf{G}_2^{(\tau)}$ as unitary 2×2 matrices on the form

$$\mathbf{G}_1^{(\tau)} = \begin{bmatrix} w & z \\ -z^* e^{j\theta_\tau} & w^* e^{j\theta_\tau} \end{bmatrix}, \quad \mathbf{G}_2^{(\tau)} = \begin{bmatrix} x & y \\ -y^* e^{j\theta_\tau} & x^* e^{j\theta_\tau} \end{bmatrix},$$

$$x = \frac{1}{\sqrt{2}} e^{j\varphi_1}, \quad y = \frac{1}{\sqrt{2}} e^{j\varphi_2}, \quad z = \frac{1}{\sqrt{2}} e^{j\varphi_3}, \quad w = \frac{1}{\sqrt{2}} e^{j\varphi_4}$$

where $\varphi_1 = 1.1051$, $\varphi_2 = -1.7482$, $\varphi_3 = 2.9750$, $\varphi_4 = 0.9596$, θ_τ are linearly spaced in the interval $[0, 2\pi]$, and $\tau = 1, 2, \dots, 40$. Notice how the variation among the 40 surrogate

models displayed in Fig. 1, for $N_s = 3, 9, 12$, decreases as the number of available samples increases.

When the method proposed here is used in the benchmarking cases of Section IV, 6 randomly generated matrices of appropriate size are used (3 \mathbf{G}_1 matrices and 3 \mathbf{G}_2 matrices). This method has been tested on 6 and 90 randomly generated matrices, with no observed significant change in performance observed across the tests. Hence, for the practical implementation, 6 matrices are generated in MATLAB, with $2 * \text{rand}(p, m) - 1$, where p and m are the number of rows and columns of the approximated frequency response.

E. Loewner Generating System Based Adaptive Sampling II

The here proposed method uses the condition number of the block matrix function $\Theta(s)$ (or $\bar{\Theta}(s)$) as a function of discrete frequency to sample the next frequency point.

The frequency-dependent condition number with respect to the ℓ^2 -norm is calculated as,

$$\kappa(\Theta, s'_\ell) = \|\Theta(s'_\ell)\|_2 \|\Theta(s'_\ell)^{-1}\|_2 = \|\Theta(s'_\ell)\|_2 \|\bar{\Theta}(s'_\ell)\|_2. \quad (26)$$

With the condition number as a function of discrete frequency, $\kappa(\Theta, s'_\ell)$, we sample next frequency point according to the lowest corresponding condition number, i.e.,

$$s_{N_s+1} = \arg \min_{s'_\ell} \kappa(\Theta, s'_\ell). \quad (27)$$

To efficiently calculate $\Theta(s'_\ell)$ and $\bar{\Theta}(s'_\ell)$, consider the identities.

$$(s'_\ell \mathbb{L} - \mathbb{L}\mathbf{A})^{-1} = (s'_\ell \mathbb{I} - \mathbf{A})^{-1} \mathbb{L}^{-1},$$

and

$$(s'_\ell \mathbb{L} - \mathbf{M}\mathbb{L})^{-1} = \mathbb{L}^{-1} (s'_\ell \mathbb{I} - \mathbf{M})^{-1},$$

where \mathbf{A} and \mathbf{M} are diagonal matrices, given in (7) and (8), respectively, for points such that \mathbb{L} is invertible.

IV. NUMERICAL EXAMPLES

In this section, we apply vector fitting and the Loewner framework to antenna frequency responses using both predetermined and adaptive frequency sampling algorithms. Here, the goal is to find the smallest number of frequency samples necessary to reach a certain RMSE tolerance.

When we use the Loewner framework, the surrogate models are on the form (10), with state variables calculated from (11), with $\mathbf{D} = 0$.

Due to the Theta I algorithm's dependence on a set of 6 random matrices, the method is tested 30 times (each time with a new set of 6 random matrices, in (12)) in every benchmark case. In each benchmarking graph, the RMSE span of the method is highlighted with the yellow shaded area. The median of the 30 RMSE curves is highlighted with a solid yellow curve. Additionally, for the displayed approximated relative errors using (25), a larger number of random matrices are used (typically 300). This large number of random matrices is, however, only for displaying the estimated error, and not for driving the choice of which frequency points to choose.

In each antenna benchmarking case, equidistant distributions are tested with the Loewner framework and vector fitting. These distributions are equidistant for each iteration and are not iteratively enriched from previous iterations.

A. 5G-antenna Example

In this example, we consider the frequency response of a 5G-antenna, see inset in Fig. 3, available in CST microwave studio's component library [33]. The antenna response is calculated for 400 samples in the range 20 GHz to 60 GHz, using CST's MoM solver, depicted in Fig. 3 by the dotted line marked 'True'. In order to include a rapidly changing out-of-band data set to test the methods on, the frequency band of the simulation has been extended beyond the bandwidth of the antenna.

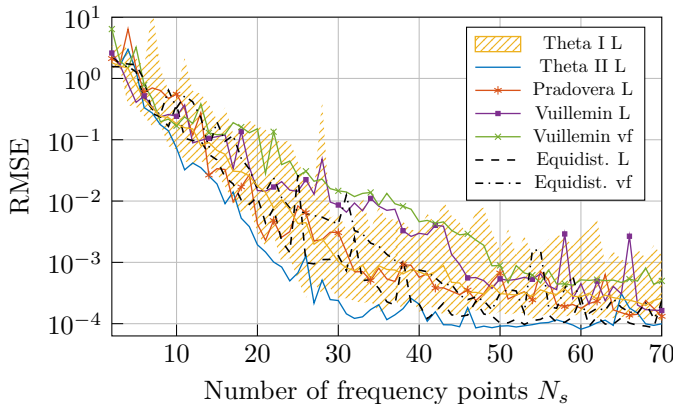


Fig. 2. RMSE (18) obtained by letting the adaptive and predetermined frequency sampling algorithms use 2 to 70 frequency points, for the 5G antenna case.

In Fig. 2, the RMSE values obtained for the adaptive sampling methods and the equidistant distributions are shown. We observe in Fig. 2 that the Loewner framework reaches a consistently lower RMSE compared to vector fitting. The

lowest RMSE is achieved by the here proposed Theta II adaptive algorithm. The Theta II algorithm is the only algorithm in Fig. 2 to distinctly outperform the equidistant distribution for the Loewner framework. Among the adaptive sampling algorithms, Theta II yields a consistently lower RMSE.

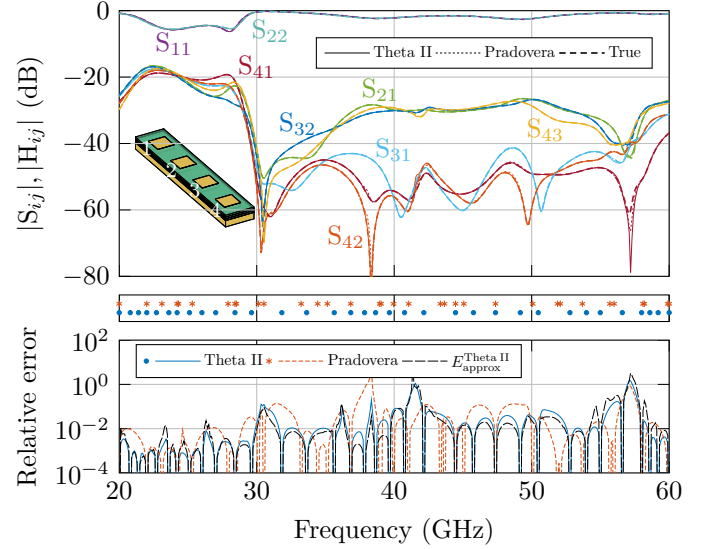


Fig. 3. In the top plot, the simulated frequency response ('true') of the 5G-antenna is displayed, as well as the surrogate models constructed using $N_s = 34$ frequency points sampled according to the Theta II and Pradovera algorithm. The middle plot shows the corresponding frequency distribution. In the bottom plot, the relative errors (19) of the surrogate models are displayed, including the approximated error (25).

The surrogate models generated using the Loewner framework yield the results displayed in Fig. 3. In order to improve readability of the plot, only a selection of scattering parameters have been plotted. For this case, 34 frequency points have been sampled using the Pradovera and Theta II algorithms, respectively. By sampling according to Theta II, the obtained overall relative error is lower, at most frequencies, than compared to sampling with the Pradovera algorithm, and all other tested adaptive methods. Additionally, the error of the Theta II generated surrogate model is accurately approximated using (25) with $N = 300$. The obtained sampling distributions using the two adaptive methods differ noticeably. A denser distribution of samples is obtained where the coupling terms are greater in magnitude for the Theta II algorithm.

B. 7×1-Vivaldi Array

For our next example, the frequency response from a 7×1 Vivaldi Array is used, see inset in Fig. 5. The frequency response is calculated for 400 samples in the range 0.5 GHz to 10 GHz, using an in-house MoM solver, and is illustrated by the dotted line in Fig. 5.

Figure 4 displays the RMSE from feeding the adaptive and predetermined methods 2 to 70 frequency points. Observing the yellow and blue lines, the corresponding methods, Theta I and II, yield similar results in terms of RMSE. The two methods perform similarly between 2 to 35 frequency points. From 35 to 57 frequency points, the Theta I method yields, on

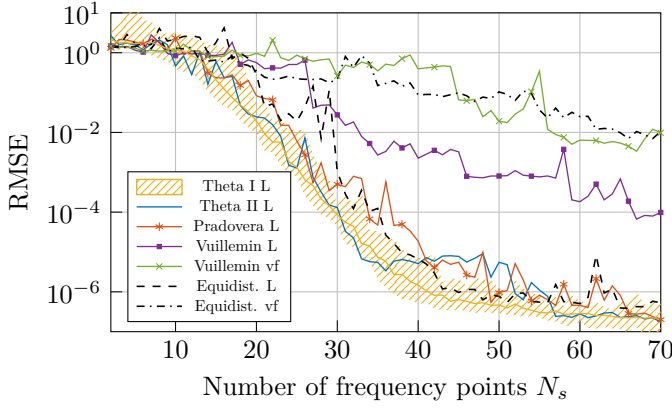


Fig. 4. RMSE obtained by letting the adaptive and predetermined frequency sampling algorithms use 2 to 70 frequency points, for the 7×1 -Vivaldi array.

average, a lower RMSE. Up until 40 frequency points, both Theta I and II outperform the equidistant distribution for the Loewner framework, whereas after 40 frequency points, only the Theta I algorithm consistently outperforms the equidistant distribution.

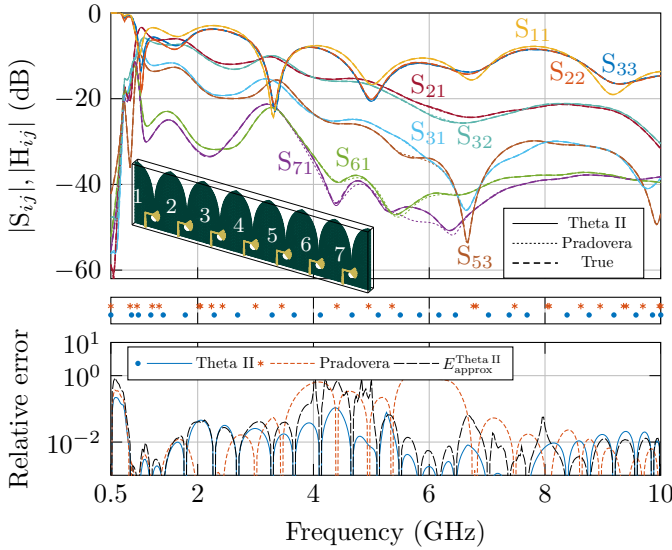


Fig. 5. In the top plot, the MoM frequency response ('true') of the Vivaldi array is displayed, as well as the surrogate models constructed using $N_s = 26$ frequency points sampled according to the Theta II and Pradovera algorithm. The middle plot shows the corresponding frequency distribution. In the bottom plot, the relative errors of the surrogate models are displayed, including the approximated error.

In Fig. 5, the surrogate models generated using the Loewner framework with 26 frequency points sampled according to the Pradovera algorithm and Theta II are shown. Only a small selection of scattering parameters are plotted to improve visibility. Among the selected scattering parameters, the most difficult to approximate are included. The corresponding relative errors between the true frequency response and the surrogate models, as well as the approximated error, are plotted below the sample distribution of the two methods.

The relative error corresponding to the Pradovera algorithm is observed to be considerably fluctuate compared to the

relative error corresponding to the Theta II algorithm. Near 6 GHz for the S_{71} parameter, the errors of the surrogate model corresponding to the Pradovera algorithm become visible. The sensitive approach of (27) minimizes such occurrences for the here proposed algorithm. Apart from these errors, both the Pradovera and Theta II algorithm generated models show good agreement with the true response. Additionally, the relative error of the Theta II generated surrogate model is accurately approximated using (25) with $N = 300$.

C. 8×2 T-Slot Loaded Dipole Array

For the next-to-last benchmarking example, we use the frequency response of a 8×2 T-slot loaded dipole array, see inset of Fig. 7. The antenna element used in this example is fully metallic, unlike the original T-slot loaded dipole element from [34]. The frequency response is calculated using an in-house MoM solver for 400 samples in the range 0.5 GHz to 15 GHz, and can be seen in Fig. 7. The frequency band of the simulation has been extended beyond the bandwidth of the antenna to provide rapidly changing out-of-band data to test the methods on.

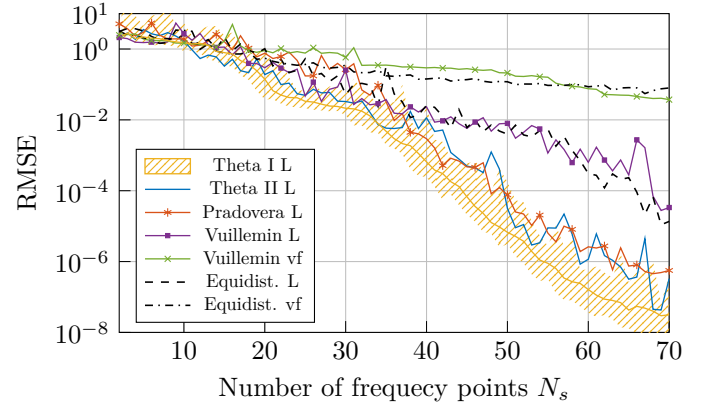


Fig. 6. RMSE obtained by letting the adaptive and predetermined frequency sampling algorithms use 2 to 70 frequency points, for the 8×2 T-slot loaded dipole array.

In Fig. 6, the RMSE of the sampling methods is displayed. The Theta I algorithm yields a noticeably smaller RMSE for the same number of frequency points used compared to the other methods. The three adaptive methods, Theta I, Pradovera and Theta II, are observed to yield a distinctly lower RMSE than any predetermined distribution (after 40 frequency points used). The difference in performance between the Loewner framework and vector fitting is also clear.

Figure 7 shows the surrogate models generated from using the Loewner framework with 35 frequency points sampled according to the Theta I and Pradovera algorithm. To increase visibility, only a selection of scattering parameters have been plotted, among them the most difficult to approximate. In the lower plot of Fig. 7, the relative errors between the surrogate models and the true frequency response are displayed, as well as the approximated error. Comparing the relative errors corresponding to the two methods, the relative error corresponding to the Pradovera algorithm is considerably greater in the 6.5

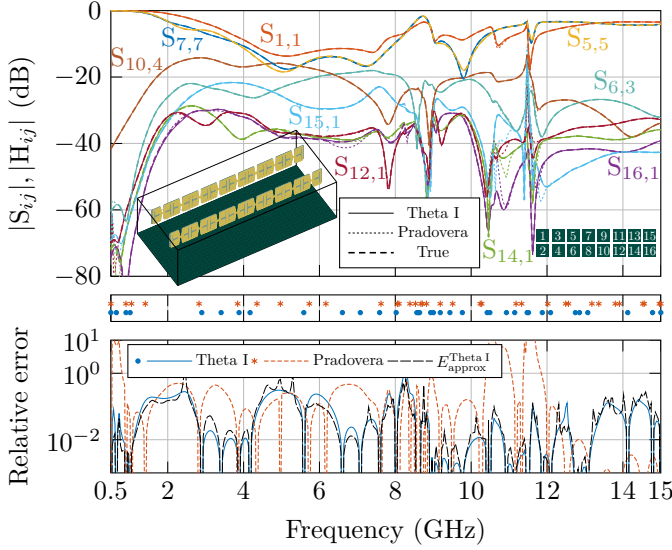


Fig. 7. In the top plot, the MoM frequency response ('true') of the T-slot loaded dipole array is displayed, as well as the surrogate models constructed using $N_s = 35$ frequency points sampled according to the Theta I and Pradovera algorithm. The middle plot shows the corresponding frequency distribution. In the bottom plot, the relative errors of the surrogate models are displayed, including the approximated error.

and 10.5 GHz range, which yields visible errors in the model. These errors occur for responses below -40 dB in absolute magnitude. The relative error corresponding to the Theta I algorithm is in contrast smoother. Additionally, the relative error of the Theta I generated surrogate model is accurately approximated using (25) with $N = 300$.

D. 4×3 BoR Array

For the last benchmarking example, we use the frequency response of a 4×3 BoR array, see inset of Fig. 9, where the BoR element is from [35]. The frequency response is calculated for 300 samples in the range 4 GHz to 20 GHz, using an in-house MoM solver. The frequency response of the BoR array is depicted by the dashed lines in Fig. 9.

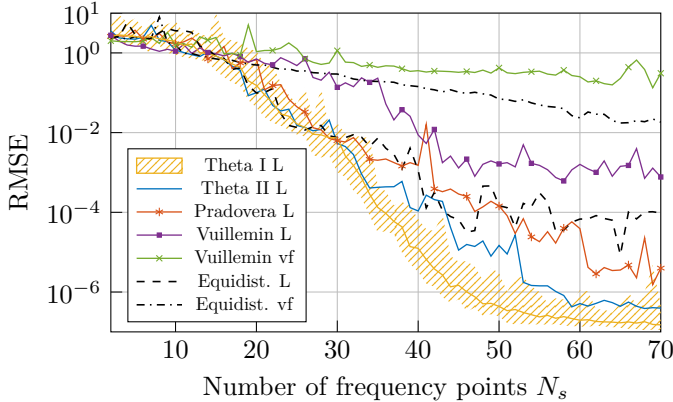


Fig. 8. RMSE obtained by letting the adaptive and predetermined frequency sampling algorithms use 2 to 70 frequency points, for the 4×3 BoR array.

Figure 8 displays the RMSE of the predetermined and adaptive sampling methods for the BoR array case. Up until

30 frequency points, the Theta I, Theta II and Pradovera algorithms perform similarly, or better than the equidistant distribution for the Loewner framework. After 30 frequency points used, the Theta I and the Theta II algorithms distinctly outperform the equidistant distribution and the Pradovera algorithm. Of the two, the Theta I algorithm yields the lowest RMSE from 30 to 70 frequency points used.

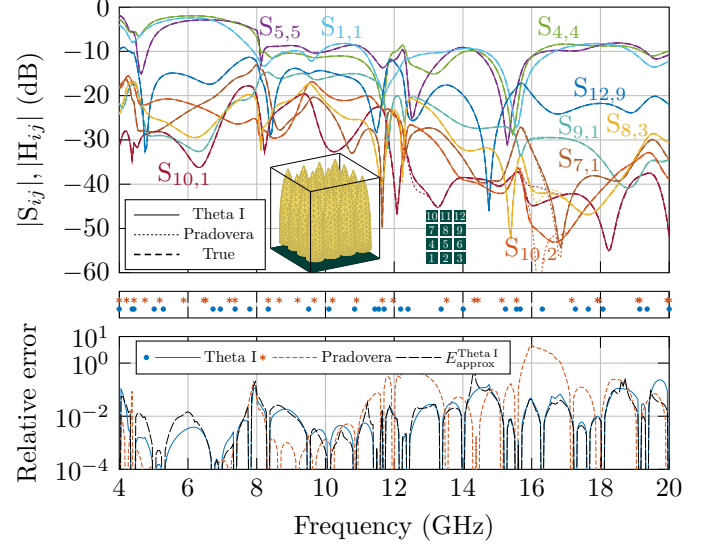


Fig. 9. In the top plot, the MoM frequency response ('true') of the BoR array is displayed, as well as the surrogate models constructed using $N_s = 30$ frequency points sampled according to the Theta I and Pradovera algorithm. The middle plot shows the corresponding frequency distribution. In the bottom plot, the relative errors of the surrogate models are displayed, including the approximated error.

In Fig. 9, we display the surrogate models constructed using the Loewner framework with 30 frequency points sampled according to the Theta I and Pradovera algorithm. Only a selection of scattering parameters have been plotted in order to increase visibility. Among the selected scattering parameters are the most difficult to approximate. The lower plot of Fig. 9 displays the corresponding relative error of the surrogate models as well as the approximated error. The surrogate models corresponding to the two methods show good agreement with the true data. Below -40 dB at 12.8 and 16 GHz, however, visible errors are observed from the model corresponding to the Pradovera algorithm, whereas the model corresponding to the Theta I algorithm shows no visible errors. Comparing the relative errors of the surrogate models corresponding to the two methods, the Theta I algorithm yields a relative error that is in contrast more smooth. Additionally, the relative error of the Theta I generated model is accurately approximated using (25) with $N = 300$.

V. CONCLUSIONS

We have proposed two novel adaptive frequency sampling algorithms, Theta I, and II, based on the Loewner generating system approach. These adaptive frequency sampling methods are used in conjunction with the Loewner framework and have been compared with other frequency sampling algorithms in

four antenna responses. Among the adaptive methods, the Theta II, Theta I, and the Pradovera algorithm succeed in sampling a minimal number of frequency points while still achieving a remarkably low RMSE in the resulting surrogate models, demonstrating their performance in maintaining accuracy with reduced computational effort. Additionally, in all of our benchmarking cases, the Loewner framework has been shown to provide the most accurate surrogate models compared to vector fitting, for all frequency sampling strategies tested in this paper.

Of the three adaptive algorithms, Theta II yields the lowest average RMSE in one of the four antenna cases (the 5G antenna), whereas the Theta I algorithm yields the lowest average RMSE in three of the four antenna cases (The Vivaldi array, the loaded dipole array, and the BoR array).

The proposed Theta I algorithm is appropriate for adaptive sampling for minimizing an error of choice. In this paper, we have used an element-wise relative difference calculation, leading to a minimization of the largest element-wise relative error. The effect of this can be seen by the smoothness of the relative error in the relative error plots of some of the benchmarking cases.

We have also shown that the proposed adaptive sampling algorithms perform better than the tested predetermined frequency sampling distributions. With the proposed adaptive sampling algorithms together with the Loewner framework, the necessary number of frequency points can be kept low while still maintaining an accurate system model.

ACKNOWLEDGMENT

This work is supported by project nr ID20-0004 from the Swedish Foundation for Strategic Research and #2022-00833 in the Strategic innovation program Smarter Electronics System, by Vinnova, Formas, Energimyn- digheten (Energy Agency), and the Swedish Research Council's Research Environment grant (SEE-6GIA 2024- 06482) for research on sixth-generation wireless systems (6G), which we gratefully acknowledge.

REFERENCES

- [1] A. Emadeddin and B. L. G. Jonsson, "A Fully Integrated Filtering Vivaldi Antenna With High Selectivity and Wide Out-of-Band Suppression," *IEEE Access*, vol. 12, pp. 2690–2700, 2024.
- [2] T. Dhaene, J. Ureel, N. Fache, and D. De Zutter, "Adaptive frequency sampling algorithm for fast and accurate S-parameter modeling of general planar structures," in *Proceedings of 1995 IEEE MTT-S International Microwave Symposium*, 1995, pp. 1427–1430 vol.3.
- [3] V. de la Rubia and Z. Peng, "Data-driven model order reduction via Loewner approach for fast frequency sweep in hybrid BI-FEM solution in large finite frequency selective surfaces," in *2017 IEEE MTT-S International Conference on Numerical Electromagnetic and Multiphysics Modeling and Optimization for RF, Microwave, and Terahertz Applications (NEMO)*, 2017, pp. 287–289.
- [4] A. Fenn, G. Thiele, and B. Munk, "Moment method analysis of finite rectangular waveguide phased arrays," *IEEE Transactions on Antennas and Propagation*, vol. 30, no. 4, pp. 554–564, 1982.
- [5] K. Zhao, M. Vouvakis, and J.-F. Lee, "The adaptive cross approximation algorithm for accelerated method of moments computations of EMC problems," *IEEE Transactions on Electromagnetic Compatibility*, vol. 47, no. 4, pp. 763–773, 2005.
- [6] A. C. Antoulas, I. V. Gosea, and A. C. Ionita, "Model Reduction of Bilinear Systems in the Loewner Framework," *SIAM Journal on Scientific Computing*, vol. 38, no. 5, pp. B889–B916, 2016, [_eprint: https://doi.org/10.1137/15M1041432](https://doi.org/10.1137/15M1041432).
- [7] J. D. Simard and A. Astolfi, "Loewner Functions and Model Order Reduction for Nonlinear Input-Affine Descriptor Systems," in *2021 60th IEEE Conference on Decision and Control (CDC)*, 2021, pp. 6887–6894.
- [8] S. Peik, R. Mansour, and Y. Chow, "Multidimensional Cauchy method and adaptive sampling for an accurate microwave circuit modeling," *IEEE Transactions on Microwave Theory and Techniques*, vol. 46, no. 12, pp. 2364–2371, 1998.
- [9] J. Yang and T. K. Sarkar, "Interpolation/Extrapolation of Radar Cross-Section (RCS) Data in the Frequency Domain Using the Cauchy Method," *IEEE Transactions on Antennas and Propagation*, vol. 55, no. 10, pp. 2844–2851, 2007.
- [10] B. Gustavsen and A. Semlyen, "Rational approximation of frequency domain responses by vector fitting," *IEEE Transactions on Power Delivery*, vol. 14, no. 3, pp. 1052–1061, 1999.
- [11] D. Deschrijver, M. Mrozowski, T. Dhaene, and D. De Zutter, "Macro-modeling of Multiport Systems Using a Fast Implementation of the Vector Fitting Method," *IEEE Microwave and Wireless Components Letters*, vol. 18, no. 6, pp. 383–385, 2008.
- [12] Q. Aumann and I. V. Gosea, "Practical challenges in data-driven interpolation: Dealing with noise, enforcing stability, and computing realizations," *International Journal of Adaptive Control and Signal Processing*, vol. n/a, no. n/a, 2023, [_eprint: https://onlinelibrary.wiley.com/doi/pdf/10.1002/acs.3691](https://onlinelibrary.wiley.com/doi/pdf/10.1002/acs.3691).
- [13] S. Grivet-Talocia and B. Gustavsen, *Passive Macromodeling*, ser. Wiley Series in Microwave and Optical Engineering. Nashville, TN: John Wiley & Sons, Nov. 2015.
- [14] I. V. Gosea and S. Güttel, "Algorithms for the Rational Approximation of Matrix-Valued Functions," *SIAM Journal on Scientific Computing*, vol. 43, no. 5, pp. A3033–A3054, Jan. 2021, publisher: Society for Industrial and Applied Mathematics.
- [15] B. Salarieh and H. M. J. D. Silva, "Review and comparison of frequency-domain curve-fitting techniques: Vector fitting, frequency-partitioning fitting, matrix pencil method and loewner matrix," *Electric Power Systems Research*, vol. 196, p. 107254, 2021.
- [16] S. Lefteriu and A. C. Antoulas, "A New Approach to Modeling Multiport Systems From Frequency-Domain Data," *IEEE Transactions on Computer-Aided Design of Integrated Circuits and Systems*, vol. 29, no. 1, pp. 14–27, 2010.
- [17] J. Becerra, Z. López, A. Rangel, and F. Vega, "A Comparison of Fitting Methods for Modeling the Front Door Coupling of Two Nearby Parabolic Antennas," in *2018 USNC-URSI Radio Science Meeting (Joint with AP-S Symposium)*, 2018, pp. 27–28.
- [18] M. Gustafsson, L. Jelinek, K. Schab, and M. Capek, "Unified Theory of Characteristic Modes—Part II: Tracking, Losses, and FEM Evaluation," *IEEE Transactions on Antennas and Propagation*, vol. 70, no. 12, pp. 11 814–11 824, 2022.
- [19] H.-B. Yuan, W.-T. Bao, C. H. Lee, B. F. Zinser, S. Campione, and J.-F. Lee, "A Method of Moments Wide Band Adaptive Rational Interpolation Method for High-Quality Factor Resonant Cavities," *IEEE Transactions on Antennas and Propagation*, vol. 70, no. 5, pp. 3595–3604, 2022.
- [20] H. Yuan, J. Ren, Y. Li, and L. Su, "Removing the Froissart Doublets in a Rational Interpolation for S-parameters," in *2022 IEEE 10th Asia-Pacific Conference on Antennas and Propagation (APCAP)*, 2022, pp. 1–2.
- [21] B. L. G. Jonsson, "Model Order Reduction for Parametric Dependence of Q-factor Bounds in IoT Applications," in *2024 18th European Conference on Antennas and Propagation (EuCAP)*, 2024, pp. 1–4.
- [22] N. Mutionkole and D. I. L. de Villiers, "Adaptive frequency sampling for radiation patterns and S-parameters of antennas," in *2017 11th European Conference on Antennas and Propagation (EUCAP)*, 2017, pp. 3195–3199.
- [23] —, "Multivariate Adaptive Sampling of Parameterized Antenna Responses," *IEEE Transactions on Antennas and Propagation*, vol. 65, no. 3, pp. 1073–1080, 2017.
- [24] K. Zhu, J. Wang, and S. Yang, "An Adaptive Interpolation Scheme for Wideband Frequency Sweep in Electromagnetic Simulations," *IEEE Antennas and Wireless Propagation Letters*, vol. 21, no. 3, pp. 471–475, 2022.
- [25] D. Pradovera, "Toward a certified greedy Loewner framework with minimal sampling," *Adv. Comput. Math.*, vol. 49, no. 6, Dec. 2023, place: Berlin, Heidelberg Publisher: Springer-Verlag.
- [26] P. Vuillemin and C. Poussot-Vassal, "Constructive interpolation points selection in the Loewner framework," Aug. 2021, [arXiv:2108.13042 \[cs, eess, math\]](https://arxiv.org/abs/2108.13042).
- [27] K. Cherifi, P. Goyal, and P. Benner, "A greedy data collection scheme for linear dynamical systems," *Data-Centric Engineering*, vol. 3, p. e16, 2022.

- [28] V. de la Rubia, "Physics-Based Greedy Algorithm for Reliable Fast Frequency Sweep in Electromagnetics via the Reduced-Basis Method," *IEEE Transactions on Antennas and Propagation*, vol. 70, no. 11, pp. 10 724–10 735, 2022.
- [29] A. C. Antoulas, S. Lefteriu, and A. C. Ionita, "Chapter 8: A Tutorial Introduction to the Loewner Framework for Model Reduction," in *Model Reduction and Approximation*. Philadelphia, PA: Society for Industrial and Applied Mathematics, 2017, pp. 335–376.
- [30] D. S. Karachalios, I. V. Gosea, and A. C. Antoulas, "6 The Loewner framework for system identification and reduction," in *Volume 1 System- and Data-Driven Methods and Algorithms*, P. Benner, S. Grivet-Talocia, A. Quarteroni, G. Rozza, W. Schilders, and L. M. Silveira, Eds. Berlin, Boston: De Gruyter, 2021, pp. 181–228.
- [31] A. J. Mayo and A. C. Antoulas, "A framework for the solution of the generalized realization problem," *Linear Algebra and its Applications*, vol. 425, no. 2, pp. 634–662, 2007.
- [32] J. Yang and T. K. Sarkar, "Accurate Interpolation of Amplitude-Only Frequency Domain Response Based on an Adaptive Cauchy Method," *IEEE Transactions on Antennas and Propagation*, vol. 64, no. 3, pp. 1005–1013, 2016.
- [33] Dassault Systèmes, "CST Studio Suite." [Online]. Available: <https://www.3ds.com/products/simulia/cst-studio-suite>
- [34] C. I. Kolitsidas and B. L. G. Jonsson, "Rectangular vs. equilateral triangular lattice comparison in a T-slot loaded strongly coupled dipole array," in *2014 XXXIth URSI General Assembly and Scientific Symposium (URSI GASS)*, 2014, pp. 1–4.
- [35] H. Holter, "Dual-Polarized Broadband Array Antenna With BOR-Elements, Mechanical Design and Measurements," *IEEE Transactions on Antennas and Propagation*, vol. 55, no. 2, pp. 305–312, 2007.